TRANSFORMER MODELING AS APPLIED TO DIFFERENTIAL PROTECTION

Stanley E. Zocholl, Armando Guzmán, Daqing Hou
Schweitzer Engineering Laboratories, Inc.
Pullman, Washington

ABSTRACT

This paper presents a power transformer model to evaluate differential element performance. The paper analyzes transformer energization, overexcitation, external fault, and internal fault conditions with this model. Test results with an actual transformer validate the model. The paper includes a guide for properly selecting current transformers for differential protection applications. Accurate power transformer modeling and proper current transformer selection lead us to improved transformer protection.

KEY WORDS

Transformer, Inrush, Excitation, Differential.

INTRODUCTION

The following questions arise while applying a differential relay for transformer protection:

- What is the amount of fundamental and second-harmonic current that the relay sees while energizing the power transformer?
- What is the harmonic content of the excitation current under overvoltage conditions?
- Does zero-sequence current affect the performance of the differential element?
- What is the relay operating time?
- How secure is the relay for external fault conditions?
- How do I select the proper current transformers for my application?
- Are the current transformers going to saturate with high-fault currents?

Actual transformer testing is one of the options to answer these questions. The testing approach is time consuming and expensive. Transformer modeling is a more attractive and less expensive option to answer these questions. The transformer model simulates current signals for different operating and fault conditions. We apply these signals to the differential relay to analyze its performance. We validate modeling results with actual testing with a laboratory transformer.

In addition to transformer modeling and differential protection evaluation, we present a guide for selecting CTs (current transformers) to avoid misapplications of differential protection.

TRANSFORMER MODELING

Basic Transformer Model

Figure 1 shows a simple single-phase shell-type transformer with two windings. We used a transformer bank with three single-phase transformers for testing and modeling purposes. The total flux in Winding 1 is the sum of the mutual flux (Φ) plus the Winding 1 leakage flux (ϕ_{11}). The sum of the mutual flux (Φ) plus the Winding 2 leakage flux (ϕ_{22}) determines the total flux in Winding 2.

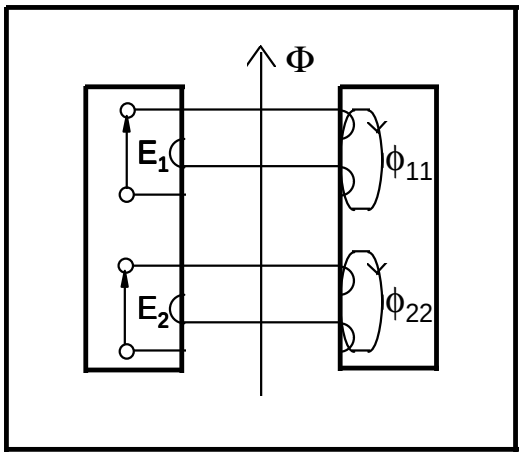

Figure 1: Single-Phase Two-Winding Transformer

The following expressions determine the relationship between voltages, currents, and mutual flux in the transformer core:

$$E_1 = R_1 \cdot I_1 + L_1 \cdot \frac{\Delta I_1}{\Delta T} + N_1 \cdot \frac{\Delta \Phi}{\Delta T} \qquad \text{Equation 1}$$

$$E_2 = R_2 \cdot I_2 + L_2 \cdot \frac{\Delta I_2}{\Delta T} + N_2 \cdot \frac{\Delta \Phi}{\Delta T} \qquad \text{Equation 2}$$

$$\Delta \Phi = P \cdot N_1 \cdot \Delta I_1 + P \cdot N_2 \cdot \Delta I_2 \qquad \text{Equation 3}$$

where:

E_1	Winding 1 input voltage, volts	L_1	Winding 1 leakage inductance, H
E_2	Winding 2 input voltage, volts	L_2	Winding 2 leakage inductance, H
I_1	Winding 1 current, amps	N_1	Winding 1 number of turns, turns
I_2	Winding 2 current, amps	N_2	Winding 2 number of turns, turns
R_1	Winding 1 resistance, Ω	ΔI	Incremental current, amps
R_2	Winding 2 resistance, Ω	$\Delta \Phi$	Incremental magnetic flux, Wb
P	Core permeance, Wb/(amp-turn)	ΔT	Incremental time, seconds

The ratio $\Delta\phi/\Delta I$ times N determines the leakage inductance (for example, $\Delta\phi_{11}/\Delta I_1$ times N_1 determines the Winding 1 leakage inductance L_1).

Equation 4 shows the matrix representation of Equations 1, 2, and 3.

$$\begin{bmatrix} E_1 - R_1 \cdot I_1 \\ E_2 - R_2 \cdot I_2 \\ 0 \end{bmatrix} = \begin{bmatrix} L_1 & 0 & N_1 \\ 0 & L_2 & N_2 \\ P \cdot N_1 & P \cdot N_2 & -1 \end{bmatrix} \cdot \begin{bmatrix} \frac{\Delta I_1}{\Delta T} \\ \frac{\Delta I_2}{\Delta T} \\ \frac{\Delta \Phi}{\Delta T} \end{bmatrix} \qquad \text{Equation 4}$$

Winding 1 and 2 voltages are the input quantities to the transformer model. We want to determine the current values for different transformer operating conditions. The first matrix in the right term of Equation 4 is the Coefficient Matrix. Equation 5 is the matrix representation of the incremental values of Winding 1 and Winding 2 currents and the incremental value of the mutual flux.

$$\begin{bmatrix} \frac{\Delta I_1}{\Delta T} \\ \frac{\Delta I_2}{\Delta T} \\ \frac{\Delta \Phi}{\Delta T} \end{bmatrix} = \begin{bmatrix} L_1 & 0 & N_1 \\ 0 & L_2 & N_2 \\ P \cdot N_1 & P \cdot N_2 & -1 \end{bmatrix}^{-1} \cdot \begin{bmatrix} E_1 - R_1 \cdot I_1 \\ E_2 - R_2 \cdot I_2 \\ 0 \end{bmatrix} \qquad \text{Equation 5}$$

All terms in the Coefficient Matrix have fixed values except the permeance P. The following expression determines the permeance of a given transformer core:

$$P = \frac{\mu \cdot A}{\ell}$$

where:

μ	Permeability, H/m
A	Transformer core area, m^2
ℓ	Mean core length, m

The ratio of the incremental value of the flux density to the incremental value of the magnetic field intensity determines the permeability μ.

$$\mu = \frac{\Delta B}{\Delta H}$$

where:

ΔB	Incremental magnetic flux density, Wb/m^2 (Tesla)
ΔH	Incremental magnetic field intensity, amp-turn/m

Figure 2 shows the well-known anhysteretic B-H curve for ferromagnetic materials with initial relative permeability $\mu_i = 15000$ and saturation flux density $B_{SAT} = 1.8$ Wb/m^2. As we can see, the permeability μ is a nonlinear function of the magnetic flux density and magnetic field intensity. The main problem when modeling transformers with an iron core is a mathematical problem. In this case, we have to solve three differential equations. We solve these equations with the fifth-order Runge-Kutta numerical method [1].

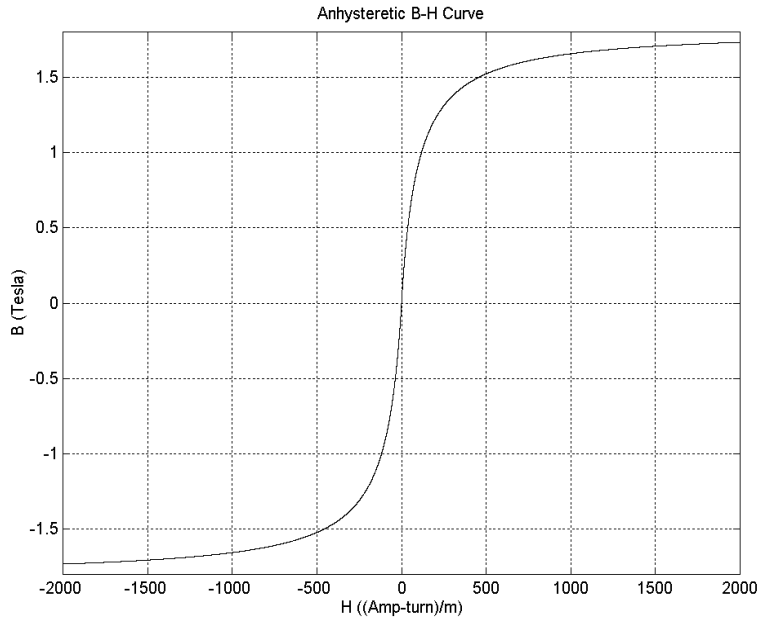

Figure 2: Anhysteretic B-H Curve of Ferromagnetic Materials with μ_i = 15000 and B_{SAT} = 1.8 Wb/m^2

The empirical Frolich Equation (Equation 6) models the S shape of the anhysteretic B-H curve [2].

$$B = \frac{H}{c + b \cdot |H|} \qquad \text{Equation 6}$$

where:

B	Magnetic flux density, Wb/m^2
H	Magnetic filed intensity, (amp-turn)/m

The following equations determine the empirical b and c constants:

$$c = \frac{1}{\mu_i \cdot \mu_0} \qquad b = \frac{1 - \frac{1}{\sqrt{\mu_i}}}{B_{SAT}}$$

where:

μ_i	Initial relative permeability
μ_0	Free space permeability
B_{SAT}	Saturation flux density

We use the anhysteretic curve modeled by the Frolich Equation to determine the permeability values for the different magnetic flux conditions presented in transformer operation.

We can model the iron core hysteresis loops using the Jiles and Atherton [3] Method. We use the Frolich Equation (Equation 6) to model the anhysteretic B-H curve instead of the Langevin Expression proposed in the original paper. Figure 3 shows the hysteresis loops using this approach. From our initial modeling studies, we found that modeling hysteresis does not improve the transformer model significantly for relay performance evaluation. We did not model

hysteresis in most of our cases. Without taking into account hysteresis, the transformer model is less complex and uses less simulation time. We can model Eddy currents with an additional third winding [4].

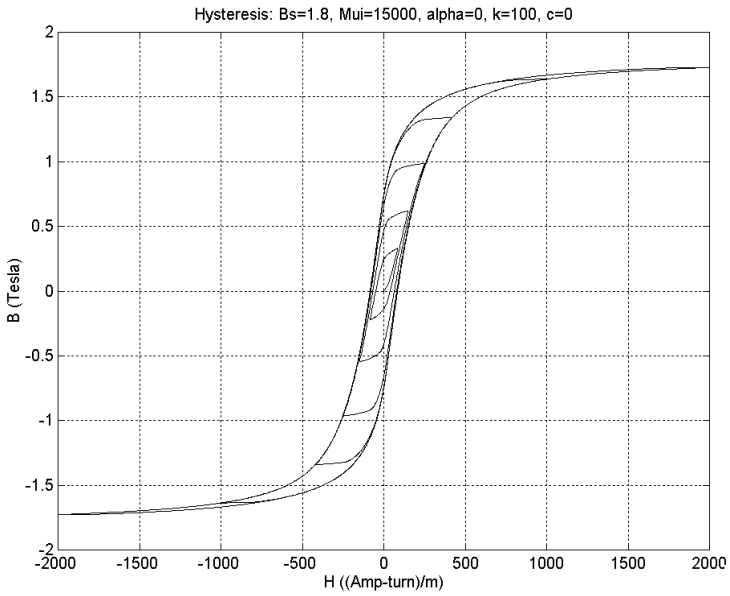

Figure 3: Hysteresis Loops Using the Jiles and Atherton Model

Figure 4 shows the basic algorithm of the transformer modeling program. We use this program to model power and current transformers. Because the primary current is known in the current transformer model, we only need to calculate the mutual flux and the secondary current. We solve two equations instead of solving Equations 1, 2, and 3.

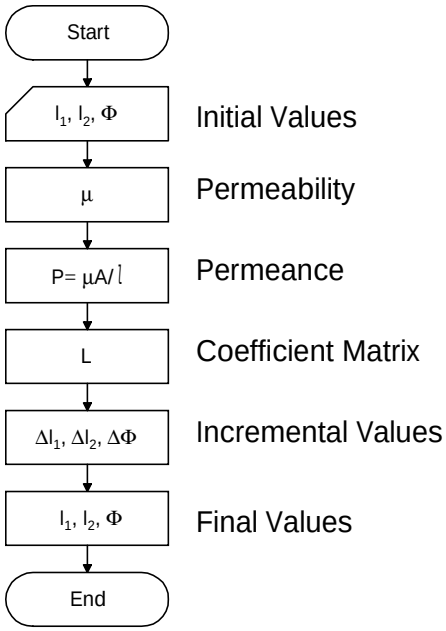

Figure 4: Transformer Model Algorithm

TRANSFORMER MODEL EVALUATION

We recorded the current signals while energizing and overexciting a laboratory transformer. Appendix A shows the laboratory transformer and power system source data that we used in the transformer model. We compared the recorded signals with the modeled signals to validate the model.

Transformer Energization

Figure 5 shows the C-phase inrush current while energizing the 15 kVA transformer bank (three 5 kVA single-phase transformers). We applied 121.24 volts to the low-voltage side of each of the single-phase transformers. The high side of the transformer was open circuited. The C-phase voltage incidence angle was zero at the time of transformer energization. The instantaneous value of the first peak of the inrush current was approximately 260 amps. The transformer nominal current is 43.5 amp rms (61.5 amp peak). The inrush peak current is approximately 4.2 times the nominal peak current. How well does the transformer model simulate this condition?

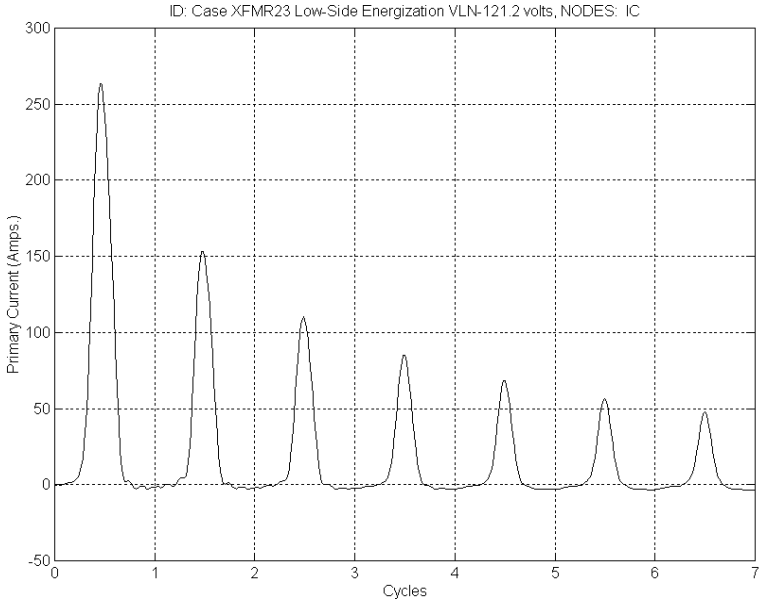

Figure 5: C-Phase Inrush Current Obtained from Transformer Testing

Figure 6 shows the C-phase inrush current obtained with the transformer model for the same conditions. As we can observe from both graphs, the current waves are similar in magnitude and in shape. The first two peaks of the inrush current are 260 and 155 amps spaced 1 cycle from each other.

The voltage incidence angle and the residual flux are main factors to determine the first peak value of the inrush current. The residual flux was zero for this energization condition. The system time constant (L/R) determines how fast the inrush current diminishes. From Appendix A, the system time constant is 6.6 ms for this condition.

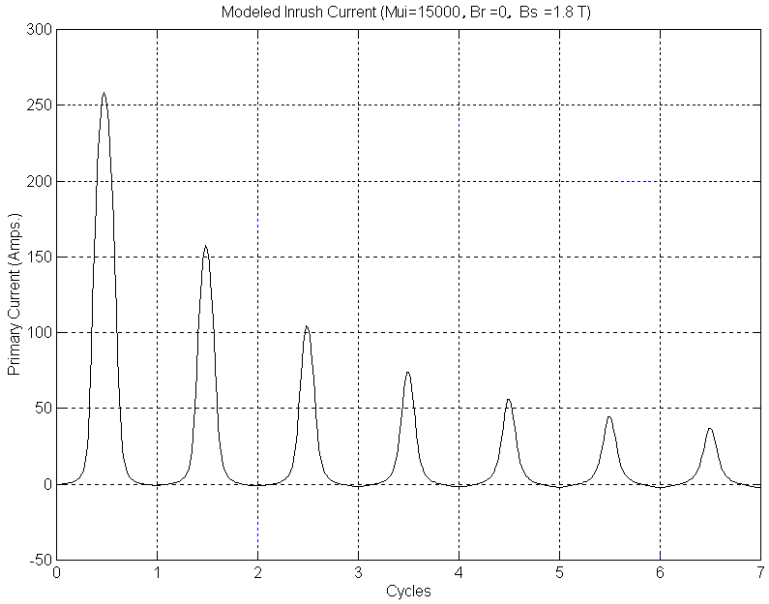

Figure 6: C-Phase Inrush Current Obtained from Transformer Modeling

Fundamental Frequency and Second-Harmonic Content of the Inrush Current

Figure 7 shows the fundamental frequency and second-harmonic content of the C-phase inrush current shown in Figure 6. The maximum fundamental frequency current magnitude is 71.9 amps, and the maximum second-harmonic magnitude is 48.0 amps. Both magnitudes decrease as the inrush current diminishes. Figure 7 also shows the second harmonic as percentage of the fundamental frequency current. This percentage is above 60% for this energization condition.

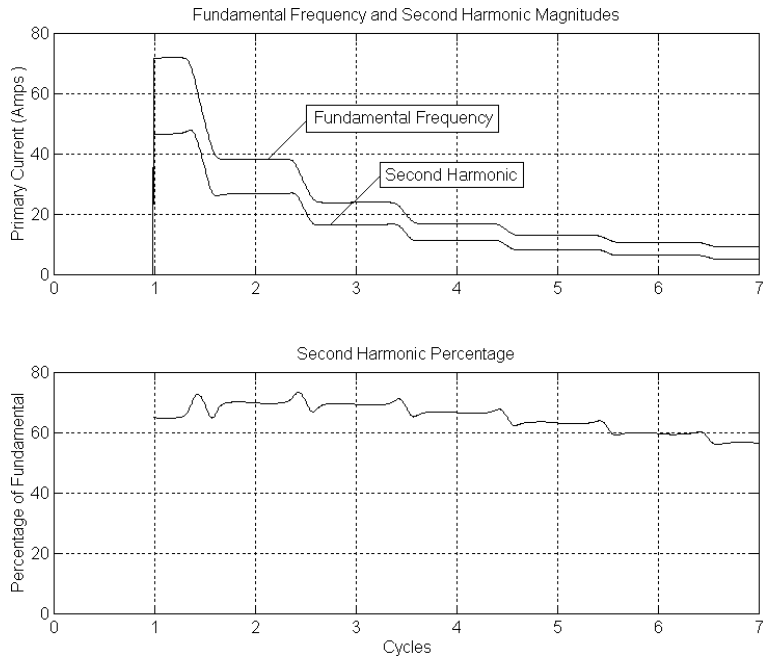

Figure 7: Fundamental Frequency and Second-Harmonic Content of the Inrush Current

Transformer Overexcitation

Figure 8 shows the A-phase excitation current that we recorded when we applied 150% overvoltage to the low-side windings of the single-phase transformer bank.

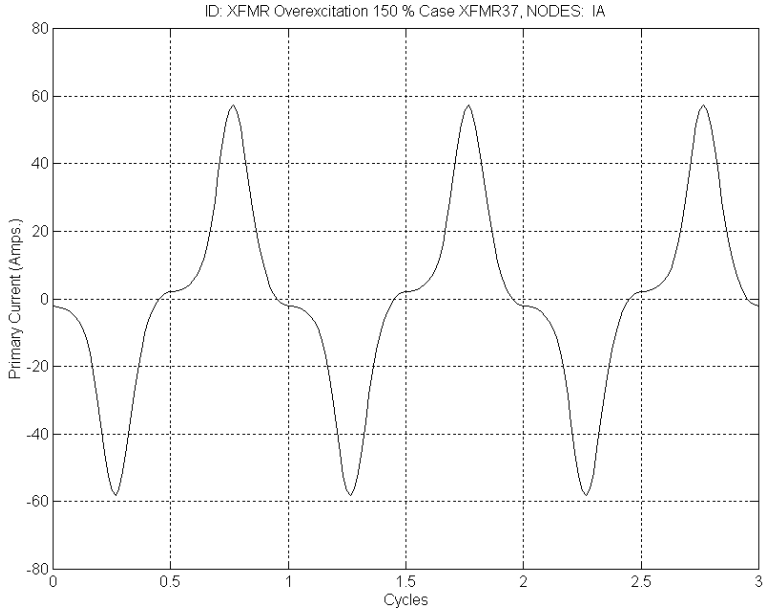

Figure 8: A-Phase Current Obtained from Transformer Testing. 150% Overvoltage on the Low Side of the Transformer

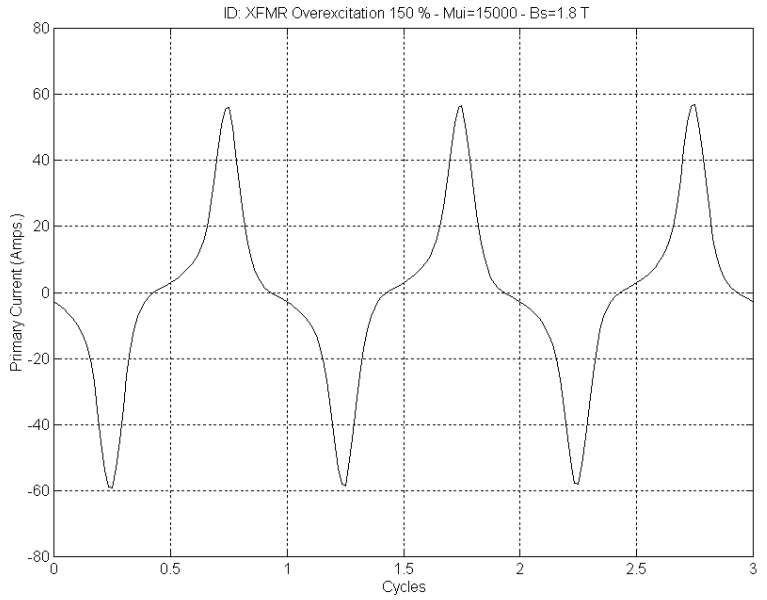

Figure 9: A-Phase Current Obtained from Transformer Modeling. 150% Overvoltage on the Low Side of the Transformer

Figure 9 shows the A-phase current obtained with the transformer model for the same overvoltage condition. The peak value of the excitation current is approximately 57 amps in the actual current and in the modeled current. The two current waves are similar in magnitude and in shape. To properly simulate the excitation current zero crossings, we modeled the hysteresis loops for this overexcitation condition.

Table 1 shows the odd-harmonic content of the current signal shown in Figure 9. The third and fifth harmonics provide reliable quantities to detect overexcitation conditions. The third harmonic is filtered out with the delta connection compensation of the differential relay or the delta connection of the CTs. A fifth-harmonic level detector can identify overexcitation conditions.

Table 1: Harmonic Content of the Excitation Current While Overexciting the Transformer Bank

Frequency Component	Magnitude (Primary Amps)	Percentage of Fundamental
Fundamental	22.5	100.0
Third	11.1	49.2
Fifth	4.9	21.7
Seventh	1.8	8.1

CURRENT DIFFERENTIAL RELAY

The relay consists of three differential elements. Each differential element provides percentage restrained differential protection with harmonic blocking and unrestrained differential protection.

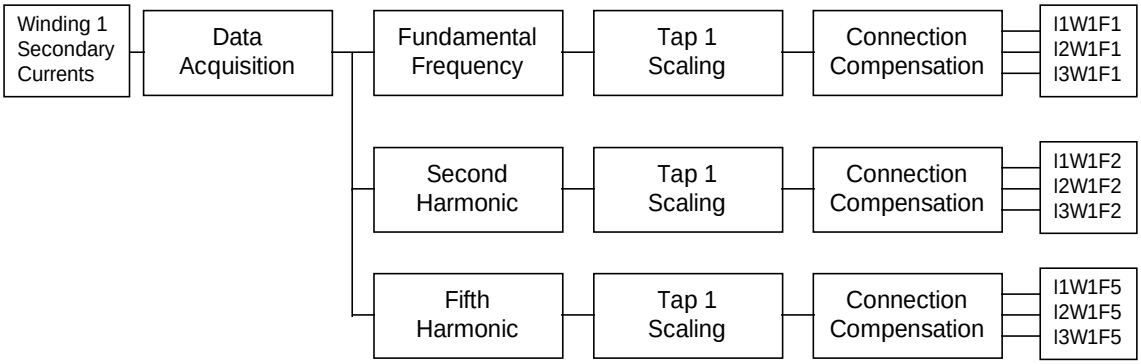

Figure 10: Data Acquisition and Filtering for Winding 1 Currents

Figure 10 shows the block diagram of the data acquisition and filtering sections for Winding 1 currents. The input currents are the CT secondary currents from Winding 1. The relay reduces the magnitude of these currents and converts them to voltage signals. Low-pass filters remove high-frequency components from the voltage signals. Digital filters extract the fundamental, second-, and fifth-harmonic quantities from the digital signals. The Tap 1 setting scales the signals in magnitude. After signal scaling, the relay removes the zero-sequence component of

the input currents and compensates the transformer phase shift if required (Appendix B describes how the relay makes the transformer connection compensation). The Winding 1 compensated currents (I1W1F1, ..., I3W1F5) are the result of relay filtering, scaling, and connection compensation. The relay obtains the Winding 2 compensated currents (I2W2F1, ..., I3W2F5) in a similar way. The three differential elements use the compensated currents from Winding 1 and 2 as inputs to their logics. For example, the Differential Element 1 uses the compensated currents I1W1F1 and I1W2F1.

Figure 11 shows the block diagram of the differential and harmonic blocking elements. The relay provides percentage restrained differential protection with harmonic blocking. The harmonic blocking elements block the restrained differential elements when the settable harmonic percentage quantity is bigger than the operating quantity.

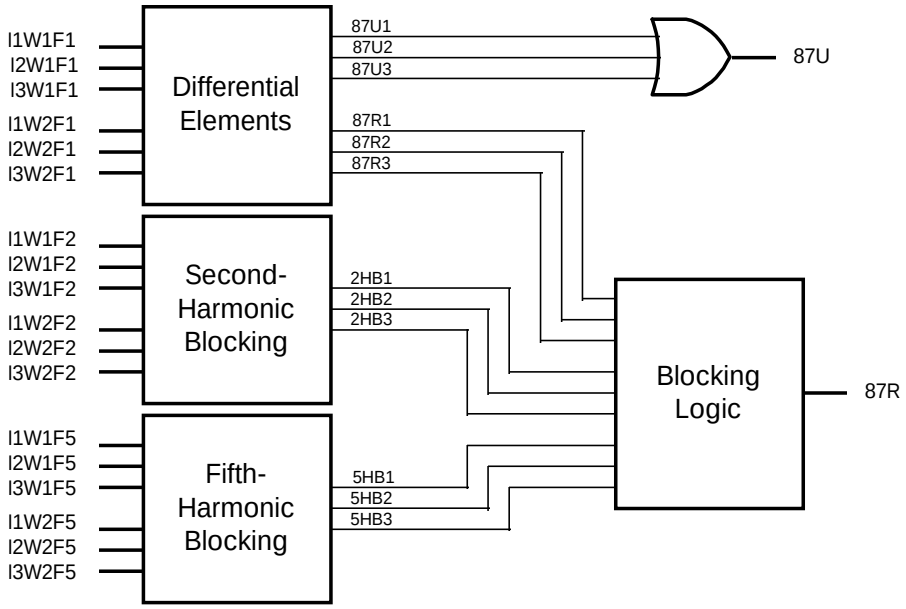

Figure 11: Differential and Blocking Elements

The magnitude of the vectorial sum of the compensated fundamental frequency currents determines the operating quantity of the restrained differential element. A settable percentage of the average of the magnitudes of the compensated currents determines the restraining quantity of this element. The relay compares the operating quantity to the restraining quantity. The percentage restrained differential element declares a tripping condition (87R element assertion) if the operating quantity is bigger than the restraining quantity and the minimum pickup level, and there is no harmonic blocking element asserted.

The relay calculates the second- and fifth-harmonic content of the differential current. It compares a settable percentage of the second- and fifth-harmonic magnitudes against the operating quantity. If the harmonic percentage is greater than the operating quantity, the harmonic blocking element asserts to block the percentage restrained differential element.

The blocking logic can operate in two ways: common harmonic blocking and independent harmonic blocking. In the common harmonic blocking mode, any harmonic blocking element (2HB1, ..., 5HB1) assertion blocks the three differential elements from operation. In the independent harmonic blocking mode, Harmonic Blocking Element 1 only blocks Differential

Element 1. The first blocking mode gives higher security than the second blocking mode. In our applications, we selected the common harmonic blocking mode. The output (87BL) of the common harmonic blocking logic is the "or" combination of the harmonic blocking elements.

The unrestrained differential element compares the operating quantity against a settable threshold. If the operating quantity is bigger than the unrestrained element threshold, the relay declares a tripping condition (87U element assertion).

DIFFERENTIAL RELAY PERFORMANCE

Differential Protection Performance while Energizing the Transformer

We tested the differential relay for different conditions upon transformer energization. We wanted to evaluate the performance of the differential elements. The transformer model simulated the input currents to the relay. Following is the relay performance for the no-fault, internal-fault, and external-fault conditions:

No-Fault Condition

Inrush currents compromise the security of differential relays. We do not want the differential relay to declare a trip condition while energizing an unfaulted transformer. The unrestrained and restrained differential elements respond to fundamental frequency only. The unrestrained differential element threshold must be set higher than the fundamental component of the highest expected inrush current. Otherwise, we must include a time delay to avoid unrestrained differential element (87U) misoperation under this condition. According to our testing results and harmonic analysis, the 87U threshold must be set above 9.0 sec. amps (71.9 pri. amps) to avoid 87U element assertion. The low-side CT ratio is 8. The typical setting for the 87U threshold is 8 times tap.

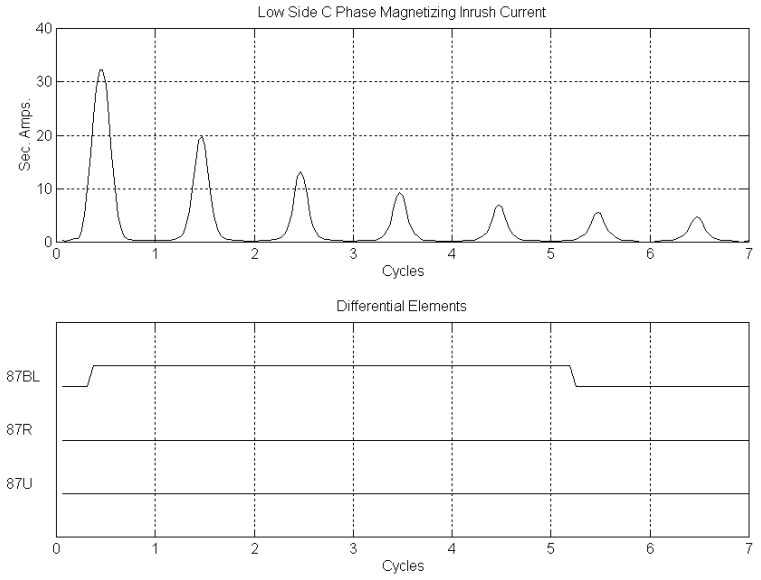

Figure 12: C-Phase Current while Energizing the 15 kVA Transformer Bank from the Low-Side

The sensitivity of the restrained differential element (87R) is higher than the unrestrained differential element. The differential relay has to detect inrush currents and disable the 87R element. The differential relay uses a settable second harmonic to fundamental percentage to block the 87R element. This percentage must be set below 60% to detect the inrush current condition shown in Figure 12. This percentage can be smaller than 60% for other transformer applications or other energization conditions. From transformer modeling and utility experience, the typical setting is 15%. Figure 7 shows the second-harmonic content as percentage of fundamental of this inrush current.

The purpose of this test was to verify that the relay second-harmonic blocking element disables the restrained differential element, and the unrestrained differential element (87U) does not assert. The single-phase transformer bank connection was wye-wye. The CT connections were wye at both sides of the transformer bank. We used the same transformer and CT connections for all the performed tests. Figure 12 shows the inrush current shown in Figure 6 in sec. amps and the 87BL, 87R, and 87U elements. The 87BL element asserts to block the restrained differential element right after the transformer energization, and the unrestrained element does not assert. The 87BL element remains asserted until the operating quantity is below the relay pickup level.

Internal-Fault Condition

What is the relay operating time for internal faults? We simulated an internal C-phase-to-ground fault in the low side of the transformer bank upon transformer energization. Figure 13 shows high-side C-phase fault current in secondary amps and the 87R element assertion. The high-side CT ratio is 4. The 87R element asserts in approximately 1.5 cycles to clear the fault.

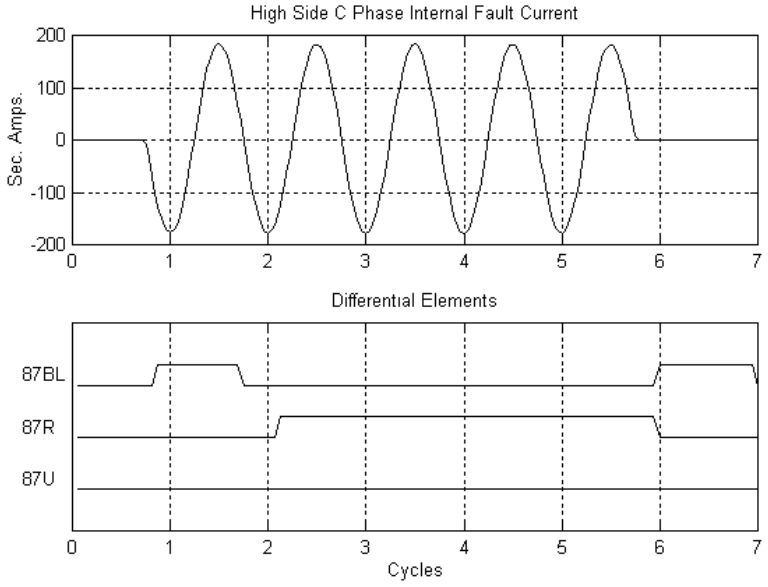

Figure 13: The Restrained Differential Element Asserts in Less than 1-1/2 Cycles to Clear the C-Phase-to-Ground Internal Fault

External-Fault Condition

How secure are the differential elements for out-of-section faults? We simulated an external C-phase-to-ground fault at the low side of the transformer bank upon transformer energization. Figure 14 shows high- and low-side C-phase secondary currents. The currents are 180° out of phase as expected for external fault conditions. The differential elements did not assert.

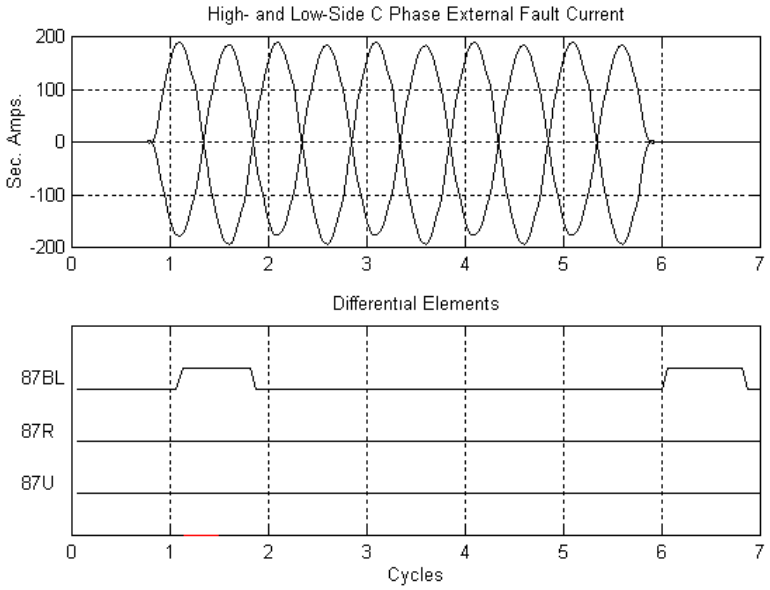

Figure 14: High- and Low-Side C-Phase Currents for an External C-Phase to Ground Fault. None of the Differential Elements Assert for the External-Fault Condition

SELECTING CTS USED WITH DIFFERENTIAL RELAYS

In transformer differential applications, CTs are selected to accommodate a maximum fault current and, at the same time, to preserve the low current sensitivity. As a minimum goal, CT saturation should be avoided for the maximum symmetrical external fault current. The CT ratio and burden capability should also permit operation of the differential instantaneous element for the maximum internal fault. The transformer application shown in Figure 15 presents a low external fault current but is complicated by the possibility of an extremely high internal fault current. The problems and solutions of this application will be made clear with simulations using CT models.

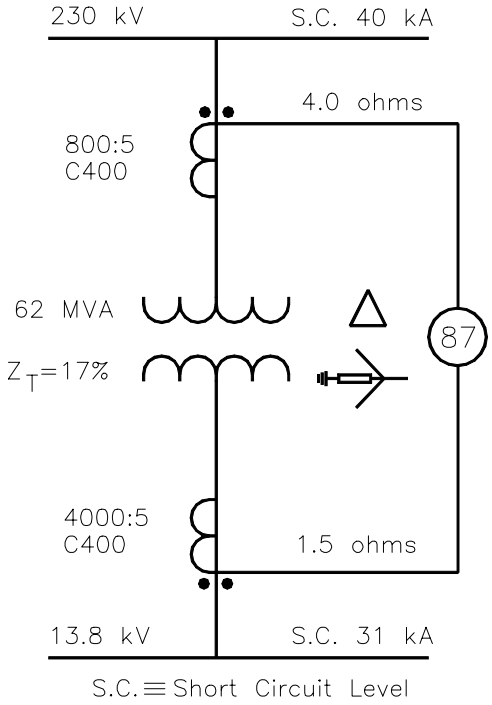

Figure 15: 62 MVA Transformer Protection Application. High-Side Short Circuit Level: 40 kA

High-Side CT Selection

A CT selection procedure is given in the forthcoming PSRC publication "Guide for the Application of Current Transformers Used for Protective Relaying Purposes." The following step-by-step procedure is given for selecting the high-side CT:

1. Select the high-side CT ratio by considering the maximum high-side continuous current I_{HS}. The choice of the CT ratio should ensure that at maximum load the continuous thermal rating of the CT, leads, and connected relay burden is not exceeded. For delta connected CTs, the relay current is $\sqrt{3}$ times the CT current. Let this ratio be the nearest standard ratio higher than I_{HS}/I_N, where I_N (relay nominal current) is 5 A or a lower value determined by the relay tap setting.

2. Determine the burden on the high-side CTs.

3. For the high-side CT ratio, select the CT accuracy class voltage that will exceed twice the product of the total high-side CT secondary burden and the maximum symmetrical CT secondary current, which could be experienced due to an external fault. If necessary, select a higher ratio than that indicated in Step 1 to meet this requirement. For the maximum internal fault, the CT ratio and burden capability should permit operation of the differential relay instantaneous unit.

From Step 1, the load current I_{HS} is 156 amps and indicates a high-side CT ratio of 200:5 for wye-connected CTs to produce a suitable relay current of 3.9 amps. The 17% transformer impedance limits the external high-side fault current to 917 amps. From Step 3, the calculated burden voltage is (917 amps / 40) (4 ohms) = 92 volts. The CT accuracy class exceeding twice this voltage is C200. The excitation curve for the C200, 200:5 CT is plotted in Figure 16. The curve shows that the rated voltage (at 10 amps of excitation current) is typically twice the excitation of the maximum permeability (located by the 45° tangent to the curve). Consequently, the burden voltage for the maximum external symmetrical fault current operates the CT at a point of maximum permeability and least error [5].

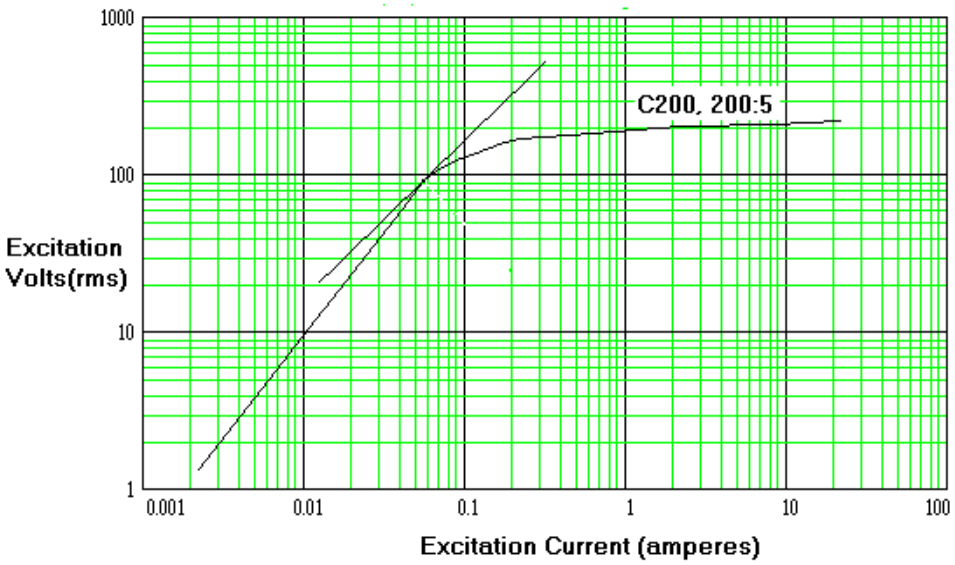

Figure 16: C200, 200:5 CT Excitation Curve

The rating is aimed at preserving sine-wave operation for symmetrical faults. It also produces a significant degree of saturation during asymmetrical faults. The magnetizing current due to CT saturation for external fault conditions appears as differential current in the relay. However, as shown in Figure 17, the relay detects the second-harmonic content of the magnetizing current and restrains differential relay tripping.

Step 3 then states that for the maximum internal fault, the ratio and burden capabilities should permit operation of the differential instantaneous unit. With a 40,000 amp internal fault current, the 200:5 CT is inadequate by inspection, and a new selection criteria is needed. In this case, the CT model will be used in conjunction with a simulation of the microprocessor digital filter algorithm to verify the operation of the instantaneous element. To preserve the current sensitivity, the CT ratio is increased to 800:5 to provide approximately one amp of secondary current at full load. The simulation of the 40,000 amp internal fault is shown in Figure 18. The simulation

shows the fundamental content of the saturated secondary current. With the instantaneous trip threshold set at 8 times tap, the trip level is reached in less than 1 cycle.

Low-Side CT Selection

A low-side CT ratio of 4000:5 provides an adequate current of 3.25 amps at full load. The burden voltage for the maximum internal fault of 16,000 amps is (16000 amps / 800)(1.5 ohms) = 30 volts. Avoiding CT saturation for the maximum asymmetrical fault requires a voltage rating of (1 + X/R) times the burden voltage for maximum symmetrical fault conditions, where X/R is the reactance to resistance ratio of the primary circuit. This criteria is met for an X/R ratio of 12 with a C400 rating as shown in the following calculation:

$$V_{rating} = \left(1 + \frac{X}{R}\right) V_{burden} = 13 \cdot 30 = 390$$

The CT ratings now provide adequate low-current sensitivity, prevent saturation on external faults, and assure operation on the extremely large internal fault currents.

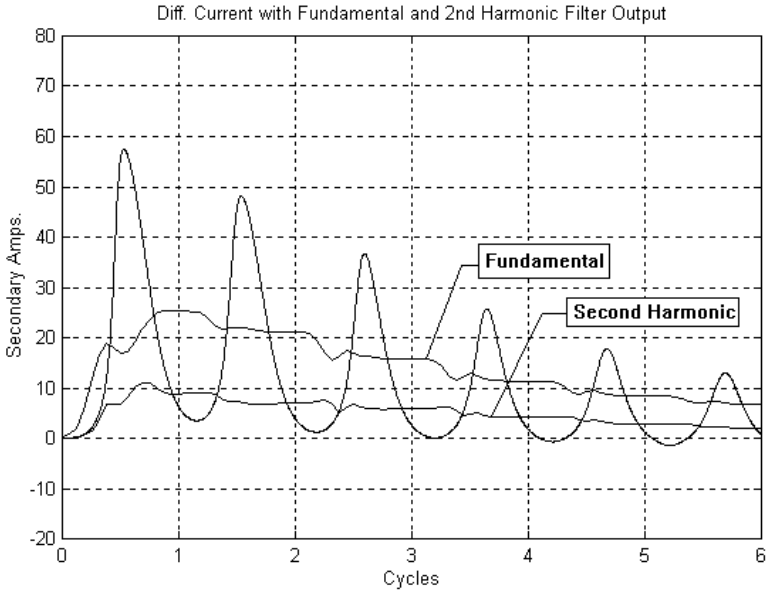

Figure 17: Difference Current Due to Magnetizing Current

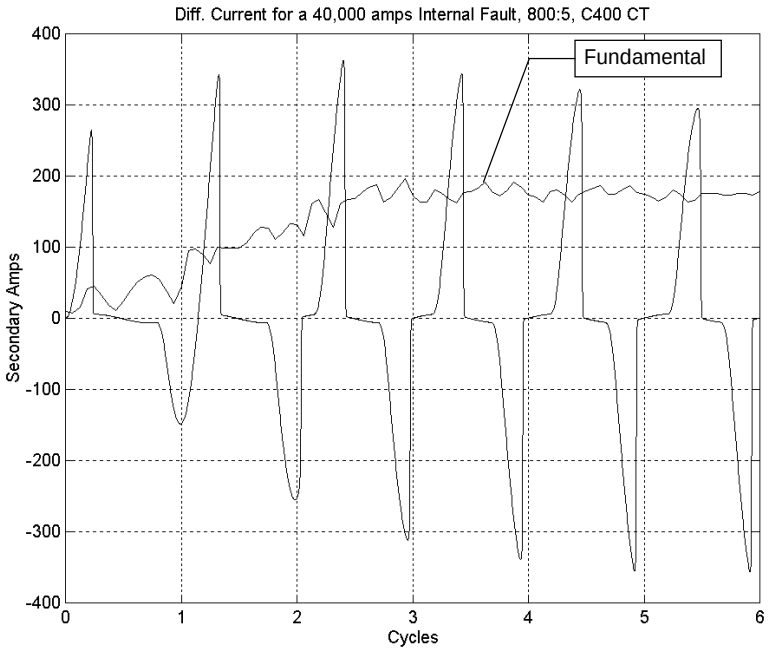

Figure 18: Secondary Current for a C400, 800:5 CT with 40,000 A Primary

CONCLUSIONS

1. Power transformer modeling is an economical way to analyze transformers for different operating conditions.

2. Using the Frolich Equation in the transformer model provides enough accuracy for differential protection evaluation purposes. Transformer models without hysteresis modeling reduce model complexity and minimize simulation time.

3. Better understanding of the harmonic content in the inrush current leads us to improved settings of the unrestrained differential element, second-harmonic blocking element, and overcurrent element.

4. A fifth-harmonic level detector can identify overexcitation conditions to block the differential element, to assert an alarm, or to trip a breaker.

5. Adequate CT selection leads us to proper transformer protection applications.

6. Digital current differential relays provide fast and reliable transformer protection. These relays give feedback for the different transformer operating conditions. This feedback was not previously available to the relay user.

REFERENCES

1. Forsythe, M. A. Malcom, and C. B. Moler, "Computer Methods for Mathematical Computations," Prentice Hall, 1977.

2. Garret, W. A. Kotheimer, and S. E. Zocholl, "Computer Simulation of Current Transformers and Relays for Performance Analysis," 14th Annual Western Protective Relay Conference, Spokane, WA, October 1990.

3. Jiles and D. L. Atherton, "Theory of Ferromagnetic Hysteresis," Journal of Magnetism and Magnetic Materials, 61 (1986) 48-60. North-Holland, Amsterdam.

4. Avila-Rosales and F. L. Alvarado, "Nonlinear Frequency Dependent Transformer Model for Electromagnetic Transient Studies in Power Systems," IEEE Transactions on Power Apparatus and Systems, Vol. PAS-101, No. 11 November 1982.

5. Zocholl and D. W. Smaha, "Current Transformer Concepts," 46th Annual Georgia Tech Protective Relay Conference, Atlanta, GA, April 1992.

6. Tuohy and J. Panek, "Chopping of Transformer Magnetizing Currents. Part I: Single Phase Transformers," IEEE Transactions on Power Apparatus and Systems, Vol. PAS-97, No. 1, January/February 1978.

APPENDIX A: TRANSFORMER AND SOURCE DATA

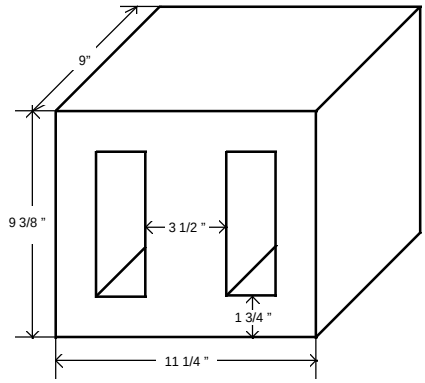

5 kVA
230/115 V
60 Hz

Figure 19: Single-Phase Shell-Type Transformer Core

Transformer data:

N_1 = 36 turns
N_2 = 18 turns
A = 0.02 m^2
ℓ = 0.58 m
L_1 = 0.24 mH
R_1 = 1.5 mΩ
L_2 = 0.06 mH
R_2 = 0.38 mΩ

Source Data:

L_S = 0.7 mH
R_S = 115 mΩ

Note: The transformer model adds the source impedance to the winding impedance.

APPENDIX B: ZERO-SEQUENCE REMOVAL AND CONNECTION COMPENSATION

In some power transformer connections, the low-side currents are not in phase with the high-side currents. For example, Figure 20 shows a transformer with delta connection in the high side and wye connection in the low side. The current in the high-side I_A-I_B leads the current in the low-side I_a by 30 ^{o}. The normal way to compensate the phase shift between the high- and low-side current is to connect the low-side CTs in delta and the high-side CTs in wye as shown in Figure 20.

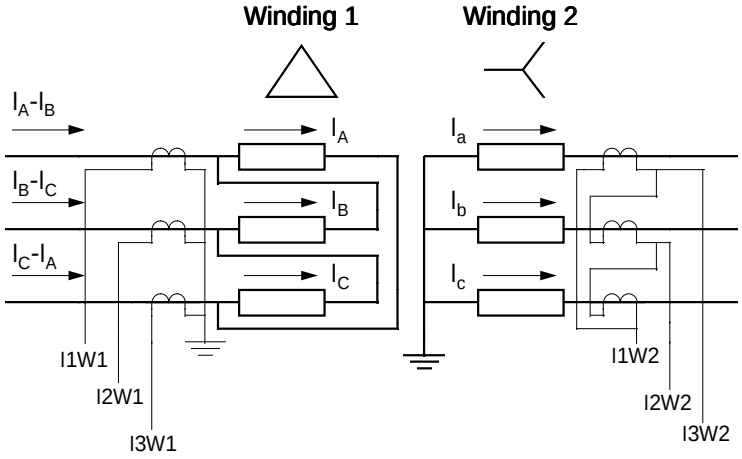

Figure 20: Delta-Wye Transformer Connection with Traditional CT connections

The Winding 1 secondary currents going into the relay are:

$$I1W1 = \frac{I_A - I_B}{CTR1} \qquad I2W1 = \frac{I_B - I_C}{CTR1} \qquad I3W1 = \frac{I_C - I_A}{CTR1}$$

The turn ratio of the power transformer is: $n = \frac{V_H}{V_L} \cdot \sqrt{3}$

where:

V_H - High-Side Voltage
V_L - Low-Side Voltage

We can express the Winding 1 secondary currents in terms of Winding 2 primary currents:

$$I1W1 = \frac{V_L}{V_H} \cdot \frac{1}{CTR1} \cdot \frac{I_a - I_b}{\sqrt{3}} = k1 \cdot \left(\frac{I_a - I_b}{\sqrt{3}} \right)$$

$$I2W1 = \frac{V_L}{V_H} \cdot \frac{1}{CTR1} \cdot \frac{I_b - I_c}{\sqrt{3}} = k1 \cdot \left(\frac{I_b - I_c}{\sqrt{3}} \right)$$

$$I3W1 = \frac{V_L}{V_H} \cdot \frac{1}{CTR1} \cdot \frac{I_c - I_a}{\sqrt{3}} = k1 \cdot \left(\frac{I_c - I_a}{\sqrt{3}} \right)$$

The Winding 2 secondary currents going into the relay are:

$$I1W2 = -\frac{1}{CTR2} \cdot \left(I_a - I_b\right) = -k2 \cdot (I_a - I_b)$$

$$I2W2 = -\frac{1}{CTR2} \cdot \left(I_b - I_c\right) = -k2 \cdot (I_b - I_c)$$

$$I3W2 = -\frac{1}{CTR2} \cdot \left(I_c - I_a\right) = -k2 \cdot (I_c - I_a)$$

The CT delta connection in Winding 2 compensates the phase shift in the power transformer and filters out the zero-sequence current component. One phase current minus the adjacent phase current (I_a - I_b) filters out zero-sequence currents.

In applications where the CTs are wye connected at the low side of the power transformer, the following current combinations compensate the power transformer phase shift and remove zero-sequence currents:

$$I1W2 = -k2 \cdot \frac{I_a - I_b}{\sqrt{3}}$$

$$I2W2 = -k2 \cdot \frac{I_b - I_c}{\sqrt{3}}$$

$$I3W2 = -k2 \cdot \frac{I_c - I_a}{\sqrt{3}}$$

The differential elements use I1W1, I2W1, I3W1, I1W2, I2W2, and I3W2 as input currents. The input currents to the differential elements do not have zero-sequence current component.